First-in-Humans Application of ^{161}Tb: A Feasibility Study Using ^{161}Tb-DOTATOC

Richard P. Baum*[1], Aviral Singh*[1,2], Harshad R. Kulkarni[1], Peter Bernhardt[3,4], Tobias Rydén[3,4], Christiane Schuchardt[1], Nadezda Gracheva[5], Pascal V. Grundler[5], Ulli Köster[6], Dirk Müller[7], Michael Pröhl[7], Jan Rijn Zeevaart[8], Roger Schibli[5,9], Nicholas P. van der Meulen[5,10], and Cristina Müller[5]

[1]*Theranostics Center for Molecular Radiotherapy and Precision Oncology, ENETS Center of Excellence, Zentralklinik Bad Berka, Bad Berka, Germany;* [2]*GROW–School for Oncology and Developmental Biology, Maastricht University Medical Center, Maastricht, The Netherlands;* [3]*Department of Radiation Physics, The Sahlgrenska Academy, University of Gothenburg, Gothenburg, Sweden;* [4]*Department of Medical Physics and Medical Bioengineering, Sahlgrenska University Hospital, Gothenburg, Gothenburg, Sweden;* [5]*Center for Radiopharmaceutical Sciences ETH-PSI-USZ, Paul Scherrer Institute, Villigen-PSI, Switzerland;* [6]*Institut Laue Langevin, Grenoble, France;* [7]*Department of Radiopharmacy, Zentralklinik Bad Berka, Bad Berka, Germany;* [8]*Radiochemistry, South African Nuclear Energy Corporation (Necsa), Pelindaba, South Africa;* [9]*Department of Chemistry and Applied Biosciences, ETH Zurich, Zurich, Switzerland; and* [10]*Laboratory of Radiochemistry, Paul Scherrer Institute, Villigen-PSI, Switzerland*

^{161}Tb has decay properties similar to those of ^{177}Lu but, additionally, emits a substantial number of conversion and Auger electrons. The aim of this study was to apply ^{161}Tb in a clinical setting and to investigate the feasibility of visualizing the physiologic and tumor biodistributions of ^{161}Tb-DOTATOC. **Methods:** ^{161}Tb was shipped from Paul Scherrer Institute, Villigen-PSI, Switzerland, to Zentralklinik Bad Berka, Bad Berka, Germany, where it was used for the radiolabeling of DOTATOC. In 2 separate studies, 596 and 1,300 MBq of ^{161}Tb-DOTATOC were administered to a 35-y-old male patient with a metastatic, well-differentiated, nonfunctional malignant paraganglioma and a 70-y-old male patient with a metastatic, functional neuroendocrine neoplasm of the pancreatic tail, respectively. Whole-body planar γ-scintigraphy images were acquired over a period of several days for dosimetry calculations. SPECT/CT images were reconstructed using a recently established protocol and visually analyzed. Patients were observed for adverse events after the application of ^{161}Tb-DOTATOC. **Results:** The radiolabeling of DOTATOC with ^{161}Tb was readily achieved with a high radiochemical purity suitable for patient application. Planar images and dosimetry provided the expected time-dependent biodistribution of ^{161}Tb-DOTATOC in the liver, kidneys, spleen, and urinary bladder. SPECT/CT images were of high quality and visualized even small metastases in bones and liver. The application of ^{161}Tb-DOTATOC was well tolerated, and no related adverse events were reported. **Conclusion:** This study demonstrated the feasibility of imaging even small metastases after the injection of relatively low activities of ^{161}Tb-DOTATOC using γ-scintigraphy and SPECT/CT. On the basis of this essential first step in translating ^{161}Tb to clinics, further efforts will be directed toward the application of ^{161}Tb for therapeutic purposes.

Key Words: ^{161}Tb; SPECT/CT imaging; DOTATOC; Auger electrons; first-in-humans

J Nucl Med 2021; 62:1391–1397
DOI: 10.2967/jnumed.120.258376

Terbium comprises 4 medically interesting radioisotopes (^{149}Tb, ^{152}Tb, ^{155}Tb, ^{161}Tb) that are potentially useful for various applications in nuclear medicine using chemically identical radiopharmaceuticals (*1*). Several years ago, the production and a preliminary preclinical application of all 4 Tb radioisotopes were demonstrated at Paul Scherrer Institute in Villigen, Switzerland (*2*). Since then, additional studies have been performed with the aims of improving production methods (*3*) and investigating the potential of these radioisotopes for nuclear imaging (^{152}Tb, ^{155}Tb) (*4*,*5*) and targeted radionuclide therapy (^{149}Tb, ^{161}Tb) (*6–10*) in more detail. In terms of clinical translation, ^{152}Tb was the only terbium radioisotope that was applied to patients in 2 independent proof-of-concept studies (*11*,*12*). ^{152}Tb-DOTATOC, a somatostatin receptor agonist, was administered to a patient with a metastatic neuroendocrine neoplasm (NEN) of the ileum at Zentralklinik Bad Berka, Bad Berka, Germany (*11*). The PET images were convincing and, because of the relatively long half-life of ^{152}Tb (17.5 h), image acquisition over an extended time period was feasible and enabled the visualization of the metastases (*11*).

^{161}Tb is, nevertheless, at the most advanced stage of all Tb radioisotopes in terms of production and preclinical investigations. This radionuclide is of particular interest for targeted radionuclide therapy because its decay properties are similar to those of ^{177}Lu (half-life of ^{161}Tb: 6.95 d (*13*); half-life of ^{177}Lu: 6.65 d) and because of the emission of medium-energy β-particles (154 keV for ^{161}Tb; 134 keV for ^{177}Lu). Importantly, ^{161}Tb emits a substantial number of conversion and Auger electrons, which are believed to make ^{161}Tb therapeutically more effective than ^{177}Lu (*14*). Several theoretic dosimetry studies consistently predicted the high potential of this radionuclide for nuclear oncology purposes (*15–20*). Preclinically, it was consistently shown that ^{161}Tb-labeled tumor-targeting agents delayed tumor growth in mice more effectively than their ^{177}Lu-labeled counterparts (*7*,*9*,*21*). It was also demonstrated in preclinical studies as well as in clinical phantom studies that ^{161}Tb can be visualized using SPECT because of the emission of γ-radiation and, thus, potentially can be used for dosimetry purposes and monitoring of the activity distribution in patients (*7*,*9*,*22*).

Received Oct. 16, 2020; revision accepted Jan. 19, 2021.
For correspondence or reprints, contact Richard P. Baum (baum@curanosticum.de) and Cristina Müller (cristina.mueller@psi.ch).
*Contributed equally to this work.
Published online February 5, 2021.

Lehenberger et al. demonstrated the concept of ^{161}Tb production using the ^{160}Gd(n,γ)^{161}Gd → ^{161}Tb nuclear reaction in analogy to the production of no-carrier-added ^{177}Lu (*14*). More recently, this production route was stepwise optimized at Paul Scherrer Institute, enabling the preparation of ^{161}Tb at a high activity and in a quality comparable to that of commercially available ^{177}Lu (*3*).

In the present study, we aimed to demonstrate first-in-humans application of ^{161}Tb-DOTATOC. After irradiation of gadolinium targets at a high-flux reactor to obtain ^{161}Tb, the ampoules were shipped to Paul Scherrer Institute, where ^{161}Tb was chemically separated from its target material. The product was transported to Zentralklinik Bad Berka, where it was directly used for the radiolabeling of DOTATOC. ^{161}Tb-DOTATOC was administered to 2 patients with NENs for whole-body planar γ-scintigraphy as well as for SPECT/CT imaging.

MATERIALS AND METHODS

Production of ^{161}Tb

^{161}Tb was produced using the ^{160}Gd(n,γ)^{161}Gd → ^{161}Tb nuclear reaction as previously reported (*3*,*14*). In brief, enriched ^{160}Gd targets were irradiated at the high-flux reactor at Institut Laue Langevin, Grenoble, France, or at the SAFARI-1 reactor at the South African Nuclear Energy Corp., Pelindaba, South Africa. ^{161}Tb was chemically separated from the gadolinium target material and other impurities as previously reported (*3*).

Radiosynthesis of ^{161}Tb-DOTATOC for Patient Application

The ^{161}Tb product was used to radiolabel DOTATOC (JPT Peptide Technologies GmbH) at Zentralklinik Bad Berka. In brief, a solution of DOTATOC (60 μg and 250 μg, for Patient 1 and Patient 2, respectively) in sodium acetate buffer (500 μL, 1 M, pH 5.5) was added to a solution of $^{161}TbCl_3$ in 0.05 M HCl (629 and 1,740 MBq for Patient 1 and Patient 2, respectively; 100 μL). The reaction mixture was incubated at 95°C for 30 min. Quality control was performed using an analytic high-pressure liquid chromatography system (Jasco PU-1580 system) equipped with a radiometric detector and a reversed-phase column (Jupiter Proteo; Phenomenex). The reaction solution was diluted with 5 mL of sterile saline and filtered using a 0.2-μm sterile filter. Samples were taken for sterility and endotoxin testing using an Endosafe-PTS cartridge (Charles River Endosafe MS, Germany). The pH of the final product was approximately 5.

Ethical and Regulatory Issues for Patient Application

^{161}Tb-DOTATOC was applied to patients in compliance with the German Medicinal Products Act (section 13, subsection 2b) and the 1964 Declaration of Helsinki (including subsequent amendments). The study was approved by an institutional review board, and the patients signed written informed consent forms before the investigation, which was performed in accordance with the regulations of the German Federal Agency for Radiation Protection (*23*). Written informed consent was obtained from the patients for collection and storage of their data in the institutional electronic data bank and for publication of the data.

Patient Selection and Characteristics

Patient 1. A 35-y-old male patient with a well-differentiated, nonfunctional malignant right glomus caroticum tumor (paraganglioma; Ki-67, 5%) and lymph node, pulmonary, hepatic, and osseous metastases was selected for this study (Table 1; Supplemental Table 1 [supplemental materials are available at http://jnm.snmjournals.org]). On diagnosis in 2011, he underwent right neck dissection, with partial excision of the primary tumor and locoregional lymphadenectomy followed by radiochemotherapy. Further partial excision of the residual tumor with lymphadenectomy was performed in early 2017. From April to July 2017, the patient received 2 cycles of intravenously

TABLE 1
Characteristics of Patients in This Study

Characteristic	Patient 1	Patient 2
Age (y)	35	70
Sex	Male	Male
Height (cm)	183	193
Body weight (kg)	94	85
Oncologic diagnosis	Metastatic, well-differentiated, nonfunctional malignant paraganglioma (initial presentation as right glomus caroticum tumor)	Metastatic, functional NEN of pancreatic tail
Metastases	Lymph node, pulmonary, hepatic, osseous	Lymph node, hepatic, pulmonary, osseous, peritoneal
Proliferation rate (Ki-67)	5%	4%
Initial diagnosis	September 2011	September 1996
Genetic predisposition	c.301G > T (p.Gly101Trp) heterozygous CDKN2A	N/A
Karnofsky Performance Score (at time of this study)	90%	80%
Previous treatments*	Surgery (2011)	Surgery (1996/2017)
	Radiochemotherapy (2011)	Chemotherapy (everolimus; 2016)
	Radionuclide therapy (2017)	Radionuclide therapy (2017)

*Detailed descriptions of previous treatments are provided in Supplemental Table 1.
N/A = not available.

applied peptide receptor radionuclide therapy using ^{177}Lu-DOTATOC. However, ^{68}Ga-DOTATOC PET/CT demonstrated progressive disease in July 2017. At the time of ^{161}Tb-DOTATOC application, the patient's Karnofsky Performance Score was 90%.

Patient 2. A 70-y-old male patient with a functional NEN of the pancreatic tail (G2) and lymph node, hepatic, pulmonary, osseous, and peritoneal metastases was selected for the (Supplemental Table 1). After initial diagnosis in 1996, partial left pancreatectomy and splenectomy followed. In 2016, he was treated with everolimus; however, this treatment was stopped because of severe stomatitis. In early 2017, the patient underwent surgical debulking of the tumor, including right hemihepatectomy, excision of hepatic segment 3, extirpation of lymph nodes in the hepatoduodenal ligament area, and tumor excision from teres as well as falciform ligaments, peritoneal adhesiolysis, and cholecystectomy. From 2005 to 2017, the patient received a total of 9 cycles of peptide receptor radionuclide therapy using either an intraarterial injection of ^{90}Y-DOTATATE or an intravenous injection of ^{177}Lu-DOTATATE or ^{177}Lu-DOTA-LM3, a somatostatin receptor antagonist. Despite these extensive treatments, the patient experienced disease progression, as demonstrated by somatostatin receptor antagonist (^{68}Ga-NODAGA-LM3)–based PET/CT. At the time of ^{161}Tb-DOTATOC application, the patient's Karnofsky Performance Score was 80%.

SPECT/CT Imaging of ^{161}Tb

SPECT/CT imaging was performed using a Siemens Symbia T camera system (Siemens Healthcare GmbH) with the following settings: low-energy high-resolution collimator, peak at 75 keV (energy window: 67.1–89.5 keV; 6% upper and lower scatter windows), 128 × 128 matrix, projections acquired with 30 s per step, step and shoot, and body contour. The numbers of projections for patients 1 and 2 were 64 and 120, respectively. The following γ-camera settings were used for planar whole-body imaging: MEDISO spirit DH-V dual-head γ-camera (Medical Imaging Systems), low-energy high-resolution collimator, peak at 49 keV (20% energy window) and peak at 77 keV (15% energy window), and scan speed of 15 cm/min. SPECT images were reconstructed with a Monte Carlo–based ordered-subset expectation maximization model using the Sahlgrenska Academy reconstruction code (*22*,*24*). The Sahlgrenska Academy reconstruction code simulates photon attenuation, scattering, and the collimator–detector resolution in the forward projection. The backprojection applies narrow-beam attenuation (without scattering). Six iterations and 4 subsets were used for all reconstructions.

Imaging of Patients After Application of ^{161}Tb-DOTATOC

Patient 1. ^{161}Tb-DOTATOC (596 MBq) was administered via a dedicated radionuclide therapy application system into a peripheral arm vein (Table 2). Ondansetron and dexamethasone were administered intravenously as premedication to prevent possible adverse effects. For nephroprotection, an amino acid solution (consisting of 1,100 mL of 5% lysine HCl, 250 mL of 10% L-arginine HCl, and 250 mL of 0.9% NaCl; pH 7.4; 400 mOsm/L) was infused intravenously over a period of 4 h, along with forced diuresis using furosemide as an intravenous bolus. After the application of ^{161}Tb-DOTATOC, 5 sets of whole-body planar (anterior and posterior) images were acquired at early time points (30 min and 3.0 h after injection), at the standard acquisition time point (24 h after injection), and at late time points (49.5 and 71 h after injection). SPECT/CT images of the thorax and of the abdomen and pelvis were acquired at 46 and 46.5 h after injection, respectively.

Patient 2. ^{161}Tb-DOTATOC (1,300 MBq) was administered using the same premedication as that described for patient 1 (Table 2). As a nephroprotective measure, diuresis was forced by the administration of furosemide, followed by adequate hydration with a balanced electrolyte solution Deltajonin (Deltamedica GmbH, Germany; 1,000 mL). After the application of ^{161}Tb-DOTATOC, 5 sets of whole-body planar (anterior and posterior) images were acquired at early time points (30 min and 2.5 h after injection), at the standard acquisition time point after 1 d (20 h after injection), and at late time points (93 and 113 h after injection). SPECT/CT of the liver and upper abdomen was performed at 19 h after injection.

The ^{161}Tb-DOTATOC SPECT/CT images were interpreted independently by 2 experienced physicians (2 board-certified nuclear medicine physicians, each with over 10 y of experience).

Dosimetry Estimation

Dosimetry was performed using planar image data from patients 1 and 2 in accordance with a previously described protocol (*25*). Time-dependent activity in the whole body and kidneys and, for patient 1,

TABLE 2
Application of ^{161}Tb-DOTATOC, Premedication, and Scan Times

Characteristic	Patient 1	Patient 2
Premedication to prevent adverse effects	Ondansetron (8 mg), intravenously	Ondansetron (8 mg), intravenously
	Dexamethasone (8 mg), intravenously	Dexamethasone (8 mg), intravenously
Measures for nephroprotection	Amino acid solution (Lys/Arg) (1,600 mL) intravenously	Electrolyte solution (1,000 mL) intravenously
	Furosemide (20 mg), intravenously	Furosemide (20 mg), intravenously
Application of ^{161}Tb-DOTATOC	596 MBq, intravenously (July 2018)	1,300 MBq, intravenously (November 2018)
Planar scans (whole body)	0.5 h after injection	0.5 h after injection
	3 h after injection	2.5 h after injection
	24 h after injection	20 h after injection
	49.5 h after injection	93 h after injection
	71 h after injection	113 h after injection
SPECT/CT scan	22.5 h after injection (thorax)	19 h after injection (liver and abdomen)
	46 h after injection (thorax)	
	46.5 h after injection (abdomen and pelvis)	

also in the liver and spleen was determined by drawing regions of interest on serial whole-body scans after the administration of ^{161}Tb-DOTATOC. The time–activity curves of source regions were fitted to exponential functions of the first or second order to determine the time-integrated activity coefficient. The mean absorbed doses were estimated with OLINDA 2.0 software.

Clinical Safety of ^{161}Tb-DOTATOC

The patients were monitored for adverse events, such as nausea, emesis, rash, erythema, pruritus, or fever, and potential changes in vital parameters, including blood pressure, pulse rate, and temperature, immediately after the ^{161}Tb-DOTATOC administration and at the follow-up review. Laboratory values, such as blood cell and relevant blood plasma parameters, were measured. The estimated glomerular filtration rate, the C-reactive protein level, and relevant tumor markers were also assessed (Supplemental Table 2).

RESULTS

Production of ^{161}Tb and Preparation of ^{161}Tb-DOTATOC

^{161}Tb was produced with product data specifications as previously defined by Gracheva et al. (*3*). The radiolabeling of DOTATOC with ^{161}Tb was performed for patient application at Zentralklinik Bad Berka to obtain ^{161}Tb-DOTATOC at a molar activity of 9.9–14.9 GBq/μmol. After incubation of the reaction mixture for 30 min at 95°C, ^{161}Tb was coordinated, and no "free" (uncoordinated) ^{161}Tb was detected by high-pressure liquid chromatography–based quality control. No microbial growth was detected in the final product when tested for sterility. The content of bacterial endotoxins in the final product was determined to be less than 10 endotoxin units/mL, in accordance with the *European Pharmacopoeia* (*26*).

First-in-Humans Application

Physiologic Biodistribution in Patient 1. Whole-body images acquired at early time points demonstrated the biodistribution of ^{161}Tb-DOTATOC within the background soft tissue, liver, spleen, and both kidneys (Figs. 1A and 1B). Accumulation of activity in the urinary bladder was due to renal excretion of ^{161}Tb-DOTATOC. At the standard image acquisition time point (24 h after injection), a moderate intensity of physiologically accumulated ^{161}Tb-DOTATOC was observed in the liver, spleen, intestines, and both kidneys, with residual activity in the bladder (Fig. 1C). Delayed images acquired 3 d after application (71 h after injection) demonstrated that ^{161}Tb-DOTATOC was continuously cleared from the normal organs and tissues (Fig. 1D). At this late time point, the spleen visually demonstrated a comparatively high accumulation of ^{161}Tb-DOTATOC (Fig. 1D). The SPECT/CT images of the thorax, abdomen, and pelvis acquired 2 d after injection demonstrated physiologic uptake of ^{161}Tb-DOTATOC in the liver, spleen, and both kidneys (Fig. 2).

Pathologic Uptake in Patient 1. Images acquired at different time points after the injection of ^{161}Tb-DOTATOC demonstrated uptake of the radiopeptide within some of the known skeletal lesions, such as the sternum and the left frontal bone, as well as in some liver lesions. The comparatively larger sternal metastasis was evident from the images obtained 3 h after injection and onward and was persistently visualized on delayed images up to 71 h after injection. The whole-body planar images acquired at 24 h after injection demonstrated distinct uptake of ^{161}Tb-DOTATOC in the relatively smaller lesion in the left orbital part of the frontal bone (Fig. 1C).

Fused SPECT/CT images of the thorax (46 h after injection) and of the abdomen and pelvis acquired 2 d after application demonstrated uptake of ^{161}Tb-DOTATOC in the osseous sternal manubrium metastasis as well as heterogeneously distributed physiologic uptake in the liver and spleen (Fig. 2).

Physiologic Biodistribution in Patient 2. Images obtained at early time points (0.5 and 2.5 h) after the injection of ^{161}Tb-DOTATOC demonstrated normal blood-pool activity, including

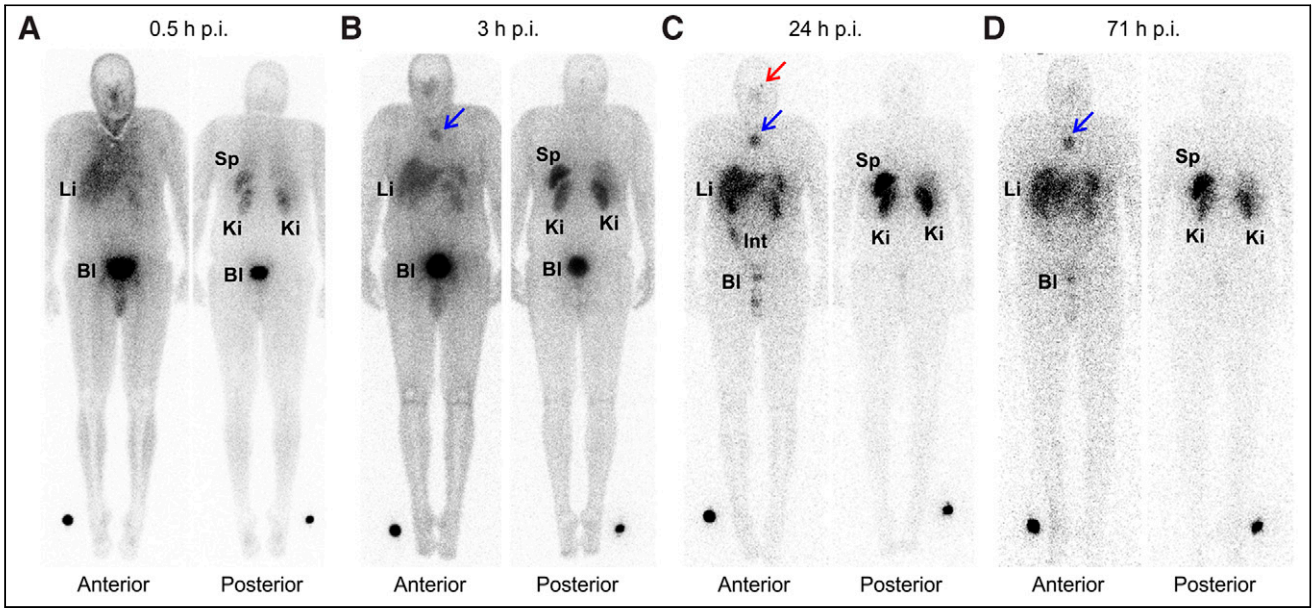

FIGURE 1. Whole-body images of patient 1 at 0.5 h after injection (A), 3 h after injection (B), 24 h after injection (C), and 3 d (71 h) (D) after injection of ^{161}Tb-DOTATOC. Images demonstrated physiologic biodistribution of ^{161}Tb-DOTATOC in liver (Li), spleen (Sp), intestines (Int), and kidneys (Ki) and excretion into urinary bladder (Bl). In addition, accumulation in known osseous metastases (sternal manubrium [blue arrows] and orbital part of frontal bone on left [red arrow]) was visualized. p.i. = after injection.

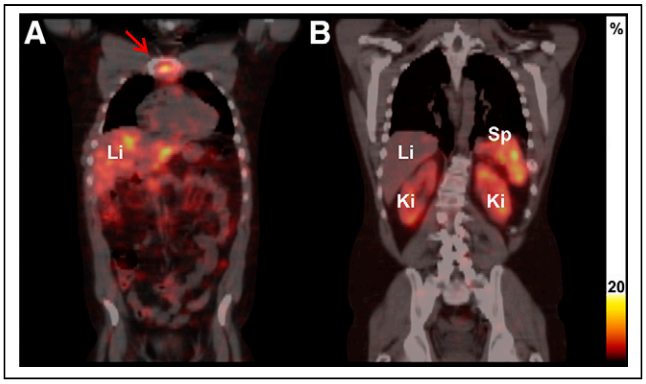

FIGURE 2. Fused coronal SPECT/CT images of patient 1 obtained on the second day after injection of ^{161}Tb-DOTATOC. Images showed pathologic uptake of ^{161}Tb-DOTATOC in osseous metastasis (sternal manubrium [red arrow]) (A) and physiologic uptake of ^{161}Tb-DOTATOC in kidneys (Ki), liver (Li), and spleen (Sp) (B).

the heart and blood vessels. Distribution of the radiopeptide was also seen in the soft tissues, liver, both kidneys, and urinary bladder (Figs. 3A and 3B). The accumulation of ^{161}Tb-DOTATOC in the kidneys and intestinal tract was observed on images obtained at 20 h after injection (Fig. 3C). The uptake of activity in the kidneys and urinary bladder was ascribed to renal excretion of ^{161}Tb-DOTATOC, as is commonly also the case for ^{177}Lu-DOTATOC. ^{161}Tb-DOTATOC was effectively cleared from normal tissues over time, as demonstrated by the reduced activity seen on images acquired at delayed time points (Fig. 3D). SPECT/CT images acquired at 19 h after injection demonstrated physiologic distribution of ^{161}Tb-DOTATOC in both kidneys as well as normal liver tissue (Fig. 4).

Pathologic Uptake in Patient 2. Whole-body planar images obtained at multiple time points demonstrated that the accumulation of ^{161}Tb-DOTATOC in bilobar hepatic metastases as early as 0.5 h after injection was still seen on images acquired at late time points (113 h after injection). Multiple skeletal metastases demonstrated faint uptake of the radiopeptide on (early) images at 2.5 h after injection of ^{161}Tb-DOTATOC, with further significant accumulation visible on images acquired at 113 h after injection (Fig. 3). SPECT/CT of the liver and upper abdomen acquired at 19 h after injection demonstrated significant accumulation of ^{161}Tb-DOTATOC in the hepatic metastases as well as moderate uptake in the multiple osseous lesions of the thoracolumbar vertebrae and the pelvis (Fig. 4).

Dosimetry Estimation

Dosimetry data from patient 1 were in a range similar to that expected when using ^{177}Lu-DOTATOC (Supplemental Table 3). Patient 2 showed slower renal clearance of ^{161}Tb-DOTATOC and, hence, higher absorbed kidney and whole-body doses (1.5 and 0.07 Gy/GBq, respectively) than patient 1 (0.8 and 0.04 Gy/GBq, respectively).

Clinical Safety of ^{161}Tb-DOTATOC

The administration of ^{161}Tb-DOTATOC and postapplication imaging procedures were well tolerated by both patients. No adverse events were reported by the patients and no significant changes in vital parameters were observed or reported by the patients during, immediately after, or at follow-up review after the administration of ^{161}Tb-DOTATOC. According to the Common Terminology Criteria for Adverse Events (CTCAE v5.0) (*27*), there were no clinically significant changes in relevant laboratory values (hematologic, renal, and hepatic panels) at the subsequent follow-up of the patients after the administration of ^{161}Tb-DOTATOC (Supplemental Table 2).

DISCUSSION

^{161}Tb was suggested for clinical translation because of its favorable physical decay properties (*16*,*18*–*20*). Importantly, ^{161}Tb can

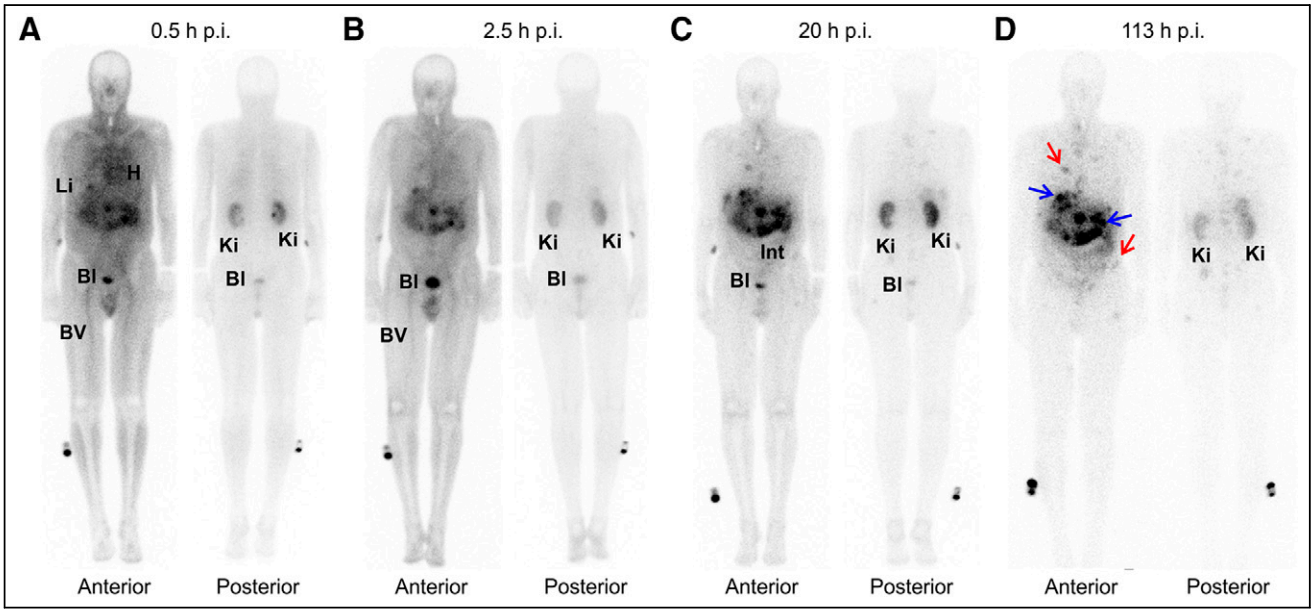

FIGURE 3. Whole-body images of patient 2 at 0.5 h after injection (A), 2.5 h after injection (B), 20 h after injection (C), and 113 h after injection (D) of ^{161}Tb-DOTATOC. Early blood-pool activity was noted in heart (H) and blood vessels (BV) up to 2.5 h after injection. Physiologic uptake of radiopeptide was observed in soft tissues, liver (Li), kidneys (Ki), intestines (Int) and urinary bladder (Bl). Pathologic accumulation of ^{161}Tb-DOTATOC was demonstrated in bilobar liver (blue arrows) and multifocal osseous metastases (red arrows). p.i. = after injection.

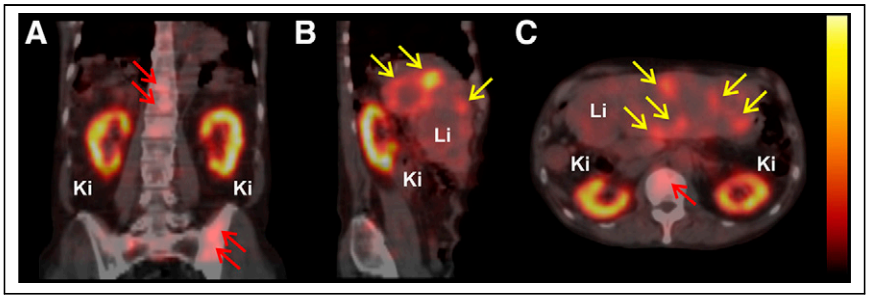

FIGURE 4. SPECT/CT images of patient 2 at 19 h after injection of ^{161}Tb-DOTATOC. (A) Coronal section. (B) Sagittal section. (C) Transverse section. Images showed uptake of ^{161}Tb-DOTATOC in bilobar hepatic metastases (yellow arrows) as well as multiple osteoblastic skeletal metastases in vertebral column and pelvis (red arrows). Physiologic uptake of ^{161}Tb-DOTATOC was seen in both kidneys (Ki) as well as in liver (Li).

be stably coordinated with a DOTA chelator because of its chemical similarity to ^{177}Lu. Therefore, it can be applied with, potentially, any tumor-targeting agent that comprises a DOTA chelator, as demonstrated in several preclinical studies (*5*,*7*,*9*,*11*).

The feasibility of using the emitted γ-radiation of ^{161}Tb for clinical SPECT was recently demonstrated with human phantoms (*22*). Low-energy high-resolution collimators were revealed to be most suited to obtaining high-resolution images, and SPECT/CT-based dosimetry was predicted to be feasible for ^{161}Tb-labeled radiopharmaceuticals (*22*). To our knowledge, the data presented in this article are the first results for ^{161}Tb clinical imaging in patients.

FIGURE 5. PET/CT sagittal section of patient 1 at 60 min after injection of ^{68}Ga-DOTATOC. Pathologic uptake was seen in multiple skeletal metastases (sternal manubrium, left orbital part of frontal bone, occipital bone, and multiple vertebrae [red arrows]). Comparatively higher physiologic uptake of ^{68}Ga-DOTATOC was observed in spleen (Sp). Accumulation of activity in urinary bladder (Bl) was seen because of renal excretion of radiopeptide.

Two patients with somatostatin receptor–expressing malignancies received ^{161}Tb-DOTATOC to analyze the distribution of the radiopeptide visualized on postapplication whole-body planar and SPECT/CT imaging. The resultant images showed a distribution profile for ^{161}Tb-DOTATOC similar to that expected for ^{177}Lu-DOTATOC. Considering that high interpatient as well as high intrapatient variations in dosimetry data are expected (*25*), the dosimetry results for the 2 patients who received ^{161}Tb-DOTATOC are of minor informative value. They confirmed, however, the expected tissue distribution of ^{161}Tb-DOTATOC. The comparatively higher absorbed kidney and whole-body doses in patient 2 can be ascribed to the slower renal clearance of ^{161}Tb-DOTATOC in this patient; the slower clearance was due to the reduced renal function demonstrated by elevated renal plasma parameters (Supplemental Table 2) (*28*).

In patient 1, despite the low administered activity of ^{161}Tb-DOTATOC, the resultant images visualized previously known osseous metastases, in agreement with visualization of the lesions on the PET/CT scan performed the previous week using ^{68}Ga-DOTATOC (Fig. 5). It is not surprising that not all of the pathologic lesions observed on ^{68}Ga-DOTATOC PET/CT images were visualized on SPECT images, which generally have lower sensitivity than high-resolution, state-of-the-art diagnostic PET/CT images. In agreement with diagnostic PET/CT images, high accumulation of ^{161}Tb-DOTATOC was found in the spleen; this was a peptide-specific feature (*29*). Patient 2 had undergone a splenectomy; consequently, the accumulation of activity in the spleen was not observed in this patient and, therefore, dosimetry data were not available.

Images acquired after the application of ^{161}Tb-DOTATOC in patient 2 demonstrated significant radiopeptide uptake in bilobar hepatic as well as multifocal osseous metastases, with visually excellent target-to-background ratios (Fig. 4). The somewhat better image quality and detection of more pathologic lesions for patient 2 were ascribed to the fact that about twice as much activity was applied in this case. Because of multiple heterogeneously distributed and difficult to delineate liver metastases in this patient, dosimetry data for the liver could not be determined.

In both patients, ^{161}Tb-DOTATOC was well tolerated, without any signs of adverse events during or after the procedure, indicating that the application of ^{161}Tb-DOTATOC is safe.

There is no doubt that ^{161}Tb holds promise as an alternative to ^{177}Lu for peptide receptor radionuclide therapy; however, it may be important to use a targeting agent that will fully exploit the short-range electron emission.

CONCLUSION

The patient images obtained with ^{161}Tb in the present study confirmed that the emitted γ-radiation of ^{161}Tb can be used for whole-body planar as well as SPECT/CT imaging of even low activities of injected ^{161}Tb. The results of the present study will serve as a basis for further investigations in patients with ^{161}Tb-based radiopharmaceuticals and a stepwise escalation of the ^{161}Tb activity applied, thereby achieving therapeutic efficacy.

DISCLOSURE

Roger Schibli, Nicholas P. van der Meulen, Cristina Müller, and Richard P. Baum received the Neuroendocrine Tumor Research Foundation (NETRF) Peterson Investigator Award 2018 (United States), which was a major contribution to the funding of this project. Peter Bernhardt and Tobias Rydén were supported by the Swedish Cancer Society, Swedish Radiation Safety Authority, King Gustav V. Jubilee Clinic Cancer Research Foundation, Swedish Research Council, and Swedish State under an agreement between the Swedish government and the county councils (the ALF agreement). No other potential conflict of interest relevant to this article was reported.

KEY POINTS

QUESTION: Is it feasible to visualize metastases in patients with NENs after injection of ^{161}Tb-DOTATOC?

PERTINENT FINDINGS: This first-in-humans application of ^{161}Tb demonstrated the feasibility of imaging metastases of NENs after the injection of relatively low activities of ^{161}Tb-DOTATOC using γ-scintigraphy and SPECT.

IMPLICATIONS FOR PATIENT CARE: The feasibility of imaging ^{161}Tb in patients is an essential finding in view of ^{161}Tb-based radionuclide therapy in future clinical trials.

ACKNOWLEDGMENTS

We thank Lebogang Sepini at Necsa for arrangements with the shipment of irradiated targets from South Africa to Switzerland. We also thank the people responsible for radiation safety, transport of radioactive materials, and technical assistance at Paul Scherrer Institute. Furthermore, we thank the nursing staff as well as the nuclear medicine technologists for patient management at Zentralklinik Bad Berka.

REFERENCES

1. Müller C, Domnanich KA, Umbricht CA, van der Meulen NP. Scandium and terbium radionuclides for radiotheranostics: current state of development towards clinical application. *Br J Radiol.* 2018;91:20180074.
2. Müller C, Zhernosekov K, Köster U, et al. A unique matched quadruplet of terbium radioisotopes for PET and SPECT and for α- and β^--radionuclide therapy: an in vivo proof-of-concept study with a new receptor-targeted folate derivative. *J Nucl Med.* 2012;53:1951–1959.
3. Gracheva N, Müller C, Talip Z, et al. Production and characterization of no-carrier-added ^{161}Tb as an alternative to the clinically-applied ^{177}Lu for radionuclide therapy. *EJNMMI Radiopharm Chem.* 2019;4:12.
4. Müller C, Fischer E, Behe M, et al. Future prospects for SPECT imaging using the radiolanthanide terbium-155: production and preclinical evaluation in tumor-bearing mice. *Nucl Med Biol.* 2014;41(suppl):e58–e65.
5. Müller C, Vermeulen C, Johnston K, et al. Preclinical in vivo application of ^{152}Tb-DOTANOC: a radiolanthanide for PET imaging. *EJNMMI Res.* 2016;6:35.
6. Müller C, Reber J, Haller S, et al. Folate receptor targeted alpha-therapy using terbium-149. *Pharmaceuticals (Basel).* 2014;7:353–365.
7. Müller C, Reber J, Haller S, et al. Direct in vitro and in vivo comparison of ^{161}Tb and ^{177}Lu using a tumour-targeting folate conjugate. *Eur J Nucl Med Mol Imaging.* 2014;41:476–485.
8. Müller C, Vermeulen C, Köster U, et al. Alpha-PET with terbium-149: evidence and perspectives for radiotheragnostics. *EJNMMI Radiopharm Chem.* 2017;1:5.
9. Müller C, Umbricht CA, Gracheva N, et al. Terbium-161 for PSMA-targeted radionuclide therapy of prostate cancer. *Eur J Nucl Med Mol Imaging.* 2019;46:1919–1930.
10. Umbricht CA, Köster U, Bernhardt P, et al. Alpha-PET for prostate cancer: preclinical investigation using ^{149}Tb-PSMA-617. *Sci Rep.* 2019;9:17800.
11. Baum RP, Singh A, Benesova M, et al. Clinical evaluation of the radiolanthanide terbium-152: first-in-human PET/CT with ^{152}Tb-DOTATOC. *Dalton Trans.* 2017;46:14638–14646.
12. Müller C, Singh A, Umbricht CA, et al. Preclinical investigations and first-in-human application of ^{152}Tb-PSMA-617 for PET/CT imaging of prostate cancer. *EJNMMI Res.* 2019;9:68.
13. Durán MT, Juget F, Nedjadi Y, et al. Determination of ^{161}Tb half-life by three measurement methods. *Appl Radiat Isot.* 2020;159:109085.
14. Lehenberger S, Barkhausen C, Cohrs S, et al. The low-energy beta$^-$ and electron emitter ^{161}Tb as an alternative to ^{177}Lu for targeted radionuclide therapy. *Nucl Med Biol.* 2011;38:917–924.
15. Bernhardt P, Benjegard SA, Kolby L, et al. Dosimetric comparison of radionuclides for therapy of somatostatin receptor-expressing tumors. *Int J Radiat Oncol Biol Phys.* 2001;51:514–524.
16. Bernhardt P, Forssell-Aronsson E, Jacobsson L, Skarnemark G. Low-energy electronemitters for targeted radiotherapy of small tumours. *Acta Oncol.* 2001;40:602–608.
17. Uusijärvi H, Bernhardt P, Rösch F, Mäcke HR, Forssell-Aronsson E. Electron- and positron-emitting radiolanthanides for therapy: aspects of dosimetry and production. *J Nucl Med.* 2006;47:807–814.
18. Hindié E, Zanotti-Fregonara P, Quinto MA, Morgat C, Champion C. Dose deposits from ^{90}Y, ^{177}Lu, ^{111}In, and ^{161}Tb in micrometastases of various sizes: implications for radiopharmaceutical therapy. *J Nucl Med.* 2016;57:759–764.
19. Champion C, Quinto MA, Morgat C, Zanotti-Fregonara P, Hindié E. Comparison between three promising β^--emitting radionuclides, ^{67}Cu, ^{47}Sc and ^{161}Tb, with emphasis on doses delivered to minimal residual disease. *Theranostics.* 2016;6:1611–1618.
20. Alcocer-Ávila ME, Ferreira A, Quinto MA, Morgat C, Hindie E, Champion C. Radiation doses from ^{161}Tb and ^{177}Lu in single tumour cells and micrometastases. *EJNMMI Phys.* 2020;7:33.
21. Haller S, Pellegrini G, Vermeulen C, et al. Contribution of Auger/conversion electrons to renal side effects after radionuclide therapy: preclinical comparison of ^{161}Tb-folate and ^{177}Lu-folate. *EJNMMI Res.* 2016;6:13.
22. Marin I, Ryden T, Van Essen M, et al. Establishment of a clinical SPECT/CT protocol for imaging of ^{161}Tb. *EJNMMI Phys.* 2020;7:45.
23. Ministry GF. Laws and regulations of radiation protection. *The Radiation Protection Act, Germany.* 2017:78.
24. Rydén T, Heydorn Lagerlof J, Hemmingsson J, et al. Fast GPU-based Monte Carlo code for SPECT/CT reconstructions generates improved ^{177}Lu images. *EJNMMI Phys.* 2018;5:1.
25. Schuchardt C, Kulkarni HR, Prasad V, Zachert C, Müller D, Baum RP. The Bad-Berka dose protocol: comparative results of dosimetry in peptide receptor radionuclide therapy using ^{177}Lu-DOTATATE, ^{177}Lu-DOTANOC, and ^{177}Lu-DOTATOC. *Recent Results Cancer Res.* 2013;194:519–536.
26. European Directorate for the Quality of Medicines & HealthCare. Bacterial endotoxins. Council of Europe. 2019. European pharmacopoeia. Strasbourg: Council of Europe, Ph. Eur. 9.0 (German ed.), 277.
27. National Cancer Institute. *Common Terminology Criteria for Adverse Events (CTCAE).* Washington, DC: U.S. Department of Health and Human Services; 2017.
28. Svensson J, Berg G, Wangberg B, Larsson M, Forssell-Aronsson E, Bernhardt P. Renal function affects absorbed dose to the kidneys and haematological toxicityduring ^{177}Lu-DOTATATE treatment. *Eur J Nucl Med Mol Imaging.* 2015;42:947–955.
29. Melis M, Kaemmerer D, de Swart J, et al. Localization of radiolabeled somatostatin analogs in the spleen. *Clin Nucl Med.* 2016;41:e111–e114.